Next-to-leading order electroweak correction to $e^+e^- \to t\bar{t}$

Bianka Meçaj
Supervised by Dr.Emi Kou

Master-2 Internship at Laboratoire de l'Accélérateur Linéaire-Theory division, Orsay, France
École Polytechnique-Université Paris-Saclay, France
ETH Zürich, Switzerland

November 13^{th}, 2017

The new results were also presented at the "Top Physics-Workshop", 7-9 June 2017, CERN, Switzerland.

Introduction

It is known that at NLO the $e^+e^- \to t\bar{t}$ receives a large EW correction compared to the QCD corrections. In this work we try to gain a better insight in the origin and consequences of this correction by using helicity-polarized initial and final states in the study of the cross section.

- Linear collider ⇒ Spin-Polarized initial states.
- Short life time of the top quark ⇒ Spin-Polarized final states.

All the calculations we present here are done using GRACE-loop system.

Outline

Tree level cross section

The SM gauge symmetry: $SU(2)_L \times U(1)_Y \times SU(3)_{color}$.
The EW sector: $SU(2)_L \times U(1)_Y$, distinguishes L and R handed *chiralities*
$\Rightarrow$ vector- axial couplings: $A_V = C_L + C_R$ & $B_A = C_L - C_R$.
Our process is $e^+e^- \to t\bar{t}$ at tree level at 500 GeV.
The Feynman diagrams that contribute at $\sigma_{tree}(e^+e^- \to t\bar{t})$:

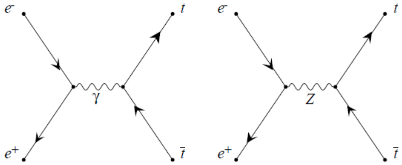

$$\mathcal{M} = \sum_{i=\gamma,Z} \frac{-ig^{\mu\nu}}{k^2 - M_i^2} \left[\bar{u}_{p_t}\gamma^\mu((A_V^i)_t - (B_A^i)_t\gamma_5)v_{p_{\bar{t}}}\right] \left[\bar{v}_{p_{e^+}}\gamma^\nu((A_V^i)_e - (B_A^i)_e\gamma_5)u_{p_{e^-}}\right]$$

$\hookrightarrow$ calculated with helicity amplitude method for different *helicity* polarizations.
The differential cross section: $\frac{d\sigma}{d\cos\theta} = 6\pi\alpha^2 \frac{1}{4s}\frac{p_t}{p_e} \mid \mathcal{M} \mid^2$

Tree level cross section

Different polarizations for the massless e^+e^-: ~~$e^+_L e^-_L$~~, ~~$e^+_R e^-_R$~~, $e^+_L e^-_R$, $e^+_R e^-_L$
and all combinations for the massive $t\bar{t}$: $t_L\bar{t}_L$, $t_R\bar{t}_R$, $t_L\bar{t}_R$, $t_R\bar{t}_L$.

Polarization	Analytic $d\sigma[pb]$	Fitting result [pb]	Error
LRLR	$0.35(1+\cos\theta)^2$	$0.35+0.70\cos\theta+0.35\cos^2\theta$	$\sim 0.1\%$
LRRL	$0.08(1-\cos\theta)^2$	$0.08-0.16\cos\theta+0.08\cos^2\theta$	$\sim 0.1\%$
LRLL	$0.09(1-\cos^2\theta)$	$0.09+0.00\cos\theta-0.09\cos^2\theta$	$\sim 0.4\%$
LRRR	$0.09(1-\cos^2\theta)$	$0.09+0.00\cos\theta-0.09\cos^2\theta$	$\sim 0.4\%$
RLLR	$0.02(1-\cos\theta)^2$	$0.02-0.05\cos\theta+0.02\cos^2\theta$	$\sim 0.1\%$
RLRL	$0.17(1+\cos\theta)^2$	$0.17+0.34\cos\theta+0.17\cos^2\theta$	$\sim 0.2\%$
RLLL	$0.04(1-\cos^2\theta)$	$0.04+0.00\cos\theta-0.04\cos^2\theta$	$\sim 0.2\%$
RLRR	$0.04(1-\cos^2\theta)$	$0.04+0.00\cos\theta-0.04\cos^2\theta$	$\sim 0.2\%$

$\hookrightarrow$ Fitting for angular distributions $\Rightarrow$ Separation of final states.

Axial-vector couplings for γ and Z

$$\sum_{j,i=\gamma,Z} [\sigma_j(A_{iV}, B_{iA}) - V_j]^2 \xrightarrow{\text{local minimum}} \textit{find } A_{iV} \textit{ and } B_{iA}.$$

Coupling	SM value	Numerical value	Error (%)
$A^t_{\gamma V}$	$\frac{2}{3}$	0.667	0.00
A^t_{ZV}	0.237	0.237	0.02
$B^t_{\gamma A}$	0	0.000	0.05
B^t_{ZA}	0.599	0.598	0.03
$A^e_{\gamma V}$	-1	-1.000	0.03
A^e_{ZV}	-0.057	-0.057	0.05
$B^e_{\gamma A}$	0	0.000	0.00
B^e_{ZA}	-0.598	-0.598	0.02

Definitions:

$$A^t_{ZV} = \frac{1}{(\sin\theta_W \cos\theta_W)}\left(\frac{1}{4} - \frac{2\sin^2\theta_W}{3}\right),\ B^t_{ZA} = \frac{1}{4\sin\theta_W\cos\theta_W},$$

$$A^e_{ZV} = \frac{1}{\sin\theta_W\cos\theta_W}\left(\frac{-1}{4} + \sin^2\theta_W\right), B^e_{ZA} = \frac{-1}{4\sin\theta_W\cos\theta_W},$$

Next - to - leading order analysis and new results.

Cross section at NLO

The cross section for $e^+e^- \to t\bar{t}$ including virtual corrections at $O(\alpha)$:

$$d\sigma_{vir} \propto | M_0 + M_{vir} |^2 = | M_0 |^2 + 2 \cdot Re\left(M_0^\dagger M_{vir}\right) + O(\alpha^2)$$

Divergences: UV & IR

UV divergences are treated with *On-shell* renormalization.

IR divergences are canceled when relevant initial & final states are summed.

$$\sigma_{NLO}\left(e^+e^- \to t\bar{t}\right) = \sigma_0 + \sigma_{vir} + \sigma_{soft} + \sigma_{hard}$$

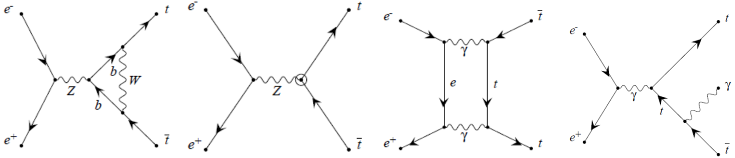

Local $SU(2) \times U(1)_Y$ symmetry $\Rightarrow$ **gauge fixing** $\Rightarrow$ Ghosts and Goldstones.

There are 150 diagrams that contribute to the $\sigma(e^+e^- \to t\bar{t})$ in the Feynman gauge(!).

Polarized cross section: high precision in $t\bar{t}X$ couplings

- Suppression of $e^-_R e^+_L \to$ **coupling effect**
  $g^i_V \propto (I^i_3 - 2Q_i \sin^2\theta_W)$, $g^i_A \propto I^i_3$
  - W boson couples only to e^-_L and e^+_R.
- Suppression of $t_L\bar{t}_L$ & $t_R\bar{t}_R$ at tree level (massless limit).
  $\Rightarrow$ Large δ_{EW}
- $\sigma_{tree}(e^-_L e^+_R \to t_L\bar{t}_R) > \sigma_{NLO}(e^-_L e^+_R \to t_L\bar{t}_R)$.

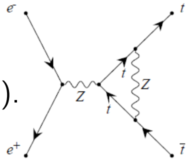

Polarization	σ_{NLO} (pb)	σ_{tree} (pb)	δ_{EW}
$e^-_L e^+_R \to t_L\bar{t}_R$	0.878	0.940	$\sim$ -7 %
$e^-_L e^+_R \to t_R\bar{t}_L$	0.241	0.216	$\sim$ 10 %
$e^-_L e^+_R \to t_L\bar{t}_L$	0.139	0.124	$\sim$ 11%
$e^-_L e^+_R \to t_R\bar{t}_R$	0.139	0.124	$\sim$ 11%
$e^-_R e^+_L \to t_R\bar{t}_L$	0.493	0.450	$\sim$ 9%
$e^-_R e^+_L \to t_L\bar{t}_R$	0.074	0.065	$\sim$ 13%
$e^-_R e^+_L \to t_L\bar{t}_L$	0.064	0.052	$\sim$ 19%
$e^-_R e^+_L \to t_R\bar{t}_R$	0.064	0.052	$\sim$ 19%

δ_{EW} for **unpolarized** $\sigma(e^+e^- \to t\bar{t})$: $\sim 3.4\%$ and δ_{EW} for $e^-_L e^+_R \to t\bar{t} \sim (-0.6\%)$

Box and Vertex corrections

- Box diagrams significant effect for $e_L^- e_R^+ \to t_L \bar{t}_R$.
- Box diagram suppressed for $e_R^- e_L^+ . \Rightarrow$ Box(W)
  - Still Box (W) $\neq 0$ for $e_L^- e_R^+ \to t_R \bar{t}_R$:
  - $P(h=+1,s)u_\uparrow = P_R \sqrt{E} \begin{bmatrix} \chi_\uparrow \\ \chi_\uparrow \end{bmatrix} + P_L \frac{m}{2E} \sqrt{E} \begin{bmatrix} \chi_\uparrow \\ -\chi_\uparrow \end{bmatrix}$
- Box & vertex cancel maximally for $e_L^- e_R^+ \to t_L \bar{t}_R$.
  $\hookrightarrow$ Reduces δ_{EW}.

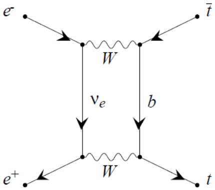

Polarization	$\sigma_{NLO}(pb)$	$M_{tree} \cdot M_{box}(pb)$	$M_{tree} \cdot M_{ver}(pb)$
$e_L^- e_R^+ \to t_L \bar{t}_R$	0.878	-0.170	0.108
$e_L^- e_R^+ \to t_R \bar{t}_L$	0.241	-0.005	0.031
$e_L^- e_R^+ \to t_L \bar{t}_L$	0.139	-0.015	0.030
$e_L^- e_R^+ \to t_R \bar{t}_R$	0.139	-0.015	0.030
$e_R^- e_L^+ \to t_R \bar{t}_L$	0.493	-0.006	0.050
$e_R^- e_L^+ \to t_L \bar{t}_R$	0.074	0.000	0.010
$e_R^- e_L^+ \to t_L \bar{t}_L$	0.064	-0.001	0.013
$e_R^- e_L^+ \to t_R \bar{t}_R$	0.064	-0.001	0.013

Forward-Backward asymmetry

Vector - Axial current $\Rightarrow$ Parity violation $\Rightarrow A_{FB} \neq 0$.

$$A_{FB} = \frac{\sigma(\frac{\pi}{2} \leq \theta \leq 0) - \sigma(\pi \leq \theta \leq \frac{\pi}{2})}{\sigma(\frac{\pi}{2} \leq \theta \leq 0) + \sigma(\pi \leq \theta \leq \frac{\pi}{2}}$$

Polarization	A_{FB} at tree level	A_{FB} at NLO
$e_L^- e_R^+ \rightarrow t_L \bar{t}_R$	0.751	0.738
$e_L^- e_R^+ \rightarrow t_R \bar{t}_L$	-0.750	-0.747
$e_L^- e_R^+ \rightarrow t_L \bar{t}_L$	0.001	0.047
$e_L^- e_R^+ \rightarrow t_R \bar{t}_R$	0.001	-0.089
$e_R^- e_L^+ \rightarrow t_R \bar{t}_L$	0.751	0.740
$e_R^- e_L^+ \rightarrow t_L \bar{t}_R$	-0.750	-0.738
$e_R^- e_L^+ \rightarrow t_L \bar{t}_L$	0.001	-0.059
$e_R^- e_L^+ \rightarrow t_R \bar{t}_R$	0.001	0.061

Table: Forward-Backward asymmetry for different polarizations

Angular distributions ($e^-_L e^+_R \to t_L \bar{t}_R$)

- **Enhancement** in the forward direction $\to$ $\sigma_{tree} \propto (1 + \cos\theta)^2$.
- The **angular distribution** is slightly **modified** :
  $0.35 + 0.70\cos\theta + 0.35\cos^2\theta \mapsto 0.34 + 0.64\cos\theta + 0.30\cos^2\theta$

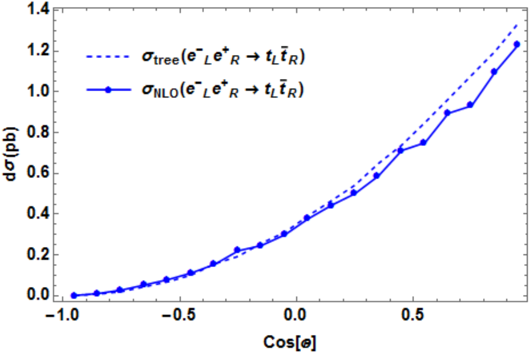

Angular distributions (other polarizations)

- **Enhancement** in the backward direction for $e^-_L e^+_R \to t_R \bar{t}_L$ and $e^-_R e^+_L \to t_L \bar{t}_R$: $\sigma_{tree} \propto (1 - \cos\theta)^2$
- Peak in $\pi/2$ for $t_L \bar{t}_L$ and $t_R \bar{t}_R$ final states: $\sigma_{tree} \propto 1 - \cos^2\theta$
- Asymmetry manifested for $e^-_L e^+_R \to t_L \bar{t}_L / t_R \bar{t}_R$.

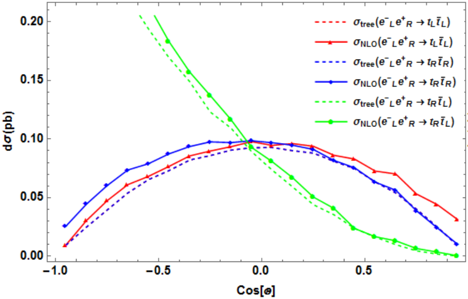

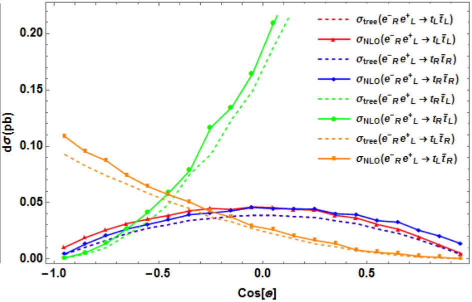

NLO distributions and W-box

Polarization	Tree distribution	NLO distribution
$LRLR$	$0.35(1+\cos\theta)^2$	$0.34+0.64\cos\theta+0.30\cos^2\theta$
$LRRL$	$0.08(1-\cos\theta)^2$	$0.09-0.18\cos\theta+0.10\cos^2\theta$
$LRLL$	$0.09(1-\cos^2\theta)$	$0.10+0.01\cos\theta-0.08\cos^2\theta$
$LRRR$	$0.09(1-\cos^2\theta)$	$0.10-0.01\cos\theta-0.09\cos^2\theta$
$RLLR$	$0.02(1-\cos\theta)^2$	$0.03-0.06\cos\theta+0.03\cos^2\theta$
$RLRL$	$0.17(1+\cos\theta)^2$	$0.17+0.37\cos\theta+0.21\cos^2\theta$
$RLLL$	$0.04(1-\cos^2\theta)$	$0.05-0.00\cos\theta-0.04\cos^2\theta$
$RLRR$	$0.04(1-\cos^2\theta)$	$0.04+0.00\cos\theta-0.04\cos^2\theta$

We find that the significant term in the W-box diagram amplitude is proportional to $(1+\cos\theta)$. But also $d\sigma_{tree}(e_L^- e_R^+) \propto (1+\cos\theta) \Rightarrow$ no contribution in modifying the distributions.

Conclusions and future perspectives

- **The study of polarized $\sigma(e^-e^+ \to t\bar{t})$ would contribute in better understanding its large δ_{EW} using spin information.**
  - $\hookrightarrow$ $e_L^- e_R^+$ initial state has the largest cross section and smallest δ_{EW}.$\rightarrow$ easier to measure.
  - $\hookrightarrow$ For $e_R^- e_L^-$ initial state and $e_L^- e_R^+ \to t_L\bar{t}_L/t_R\bar{t}_R$, the smallest cross section.$\rightarrow$ might be convenient for new physics probe.
  - $\hookrightarrow$ Cancellations between box and vertex diagrams determine the amount of the δ_{EW}.
- **The angular distribution are modified by NLO correction.**
  - $\hookrightarrow$ Experimental data fitted for σ_{NLO} instead of σ_{tree}.
  - $\hookrightarrow$ Higher precision.
  - $\hookrightarrow$ W-box diagram does not contribute in modifying the angular distributions.

For the future...

- **Study the effect of other box diagrams in modifying the angular distributions.**
- **Careful consideration on theoretical uncertainties.**
- **Study of the gauge dependence.**

Thank You!